SEMARAK ILMU PUBLISHING

Journal of Advanced Research in Applied Sciences and Engineering Technology

Journal homepage:
https://semarakilmu.com.my/journals/index.php/applied_sciences_eng_tech/index
ISSN: 2462-1943

Synthesisation, Fabrication, and Incorporation Techniques of MAX Phase and MXene Saturable Absorber in Passively Q-switched and Mode-locked All-fibre Laser Cavities: A Review

Kawther M Musthafa[1], Azura Hamzah[1,*], Ooi Wei Ling[1], Ahmad Haziq Aiman Rosol[1], Norliza Mohamed[2], Mahroof Mohamed Mafroos[3], Sulaiman Harun[4]

[1] Malaysia-Japan International Institute of Technology (MJIIT), Universiti Teknologi Malaysia, Jalan Sultan Yahya, 54100 Kuala Lumpur, Malaysia
[2] Razak Faculty of Technology and Informatics (RFTI), Universiti Teknologi Malaysia, Jalan Sultan Petra Yahya, 54100 Kuala Lumpur, Malaysia
[3] Division of Electrical and Electronic, Telecommunication Engineering Technology, Institute Technology Universiti of Moratuwa, Sri Lanka
[4] Department of Electrical Engineering, University of Malaya, Kuala Lumpur, 50603, Malaysia

ARTICLE INFO

Article history:
Received 9 June 2023
Received in revised form 29 July 2023
Accepted 1 August 2023
Available online 9 September 2023

Keywords:
MAX Phase; MXene; passively Q-switch; passively mode-lock; all-fibre laser; saturable absorber

ABSTRACT

MAX phases and MXene have been introduced in passively pulsed-laser generation for their viability as substitutes to unadventurous saturable absorbers such as saturable absorber mirror, multi-wall and single-wall carbon nanotube, graphene, and transition metal dichalcogenides, contributing to both Q-switching and mode-locking tactics. Fundamental saturable-absorber features such as nonlinear saturable absorption, astonishing depth of modulation, flexibly tuneable bandgap, and high electron density around the Fermi level, establish MAX phases and MXene as formidable contenders with decent performance in the saturable absorber regime. Recent research works contributing to MAX Phases and MXene—particularly in nonlinear ultrafast optics—have shown an exponential increase, since MAX Phases and MXene are of the prime regime of 2D nanomaterials that offer vast combination options by the formation of metal nitride, metal carbide, or carbonitride clusters with a 2D layered structure, with special emphasis on fabrication and incorporation of saturable absorbers into laser cavities. This review critically summarises the advancement on the synthesis, fabrication, and incorporation of the MAX phases and MXene saturable absorbers, as well as the incorporation methodologies and techniques into all-fibre laser cavities configured either in linear or ring configuration, summing up the identified issues and challenges and discussing future perspectives of this novel material.

1. Introduction

Pulsed all-fibre lasers have been employed in sensors [1], optical communications, digital services, spectroscopy, micromachining [2], medical systems and biomedicine [3], quantum information processing and material processing [4], and various other industries due to its unique qualities, including the ability to resist disturbance, upright the quality of beams, and high efficiency

* *Corresponding author.*
E-mail address: azurahamzah@utm.my

https://doi.org/10.37934/araset.32.2.119141

of energy conversion. Especially with pulse durations faster than a picosecond, these types of lasers have since shown further promise in a variety of other fields, including ophthalmology [5], bio-imaging [6], molecular spectroscopy and nonlinear microscopy [7]. There are a number of wavelengths in the near-infrared (NIR) area that are essentially practical; this includes the high-power ultrafast laser at 1064 nm and long-distance telephony at 1550 nm [8]. There are several approaches of producing optical pulsed lasers, mode-locking, and Q-switching, which can be characterised into two major categories: active modulation, which involves using an active modulator to control the cavity loss on a periodic basis, and passive modulation, which involves placing a saturable absorber (SA) within the laser cavity. For the creation of passive laser pulses, there are also two types of SAs in concern, one is the Kerr lens, which relies on nonlinear and/or birefringent phenomena, while the second is SA materials.

The interaction of light with SA matter is described by using nonlinear optics property. Nonlinearity, in particular, provides insight onto how materials respond to changes in the applied electromagnetic field's amplitude [9]. Saturable absorption, which has the potential to produce ultrashort pulsed lasers in the picosecond or femtosecond regimes, is one of the intriguing optical phenomena that are rapidly emerging as a result of nonlinearity effects. Intensity-dependent transmission is seen in SAs, but optical loss decreases with increasing light intensity [10]. Being a passive component, SA creates pulsed laser light through an all-fibre laser cavity's passive switching mechanism. Anticipation of the benefits regarding system size and portability, cost effectiveness, superior quality of beam, and superior heat intemperance of the fibre, the development of fibre lasers with ultrafast characteristics has attracted significant interest [11].

Out of a variety of ways reported subsequent to the initial demonstration of pulsed-lasers with femtosecond pulse-width through an intra-cavity SA dye cell—e.g., a dye laser with flashlamp-pump—in 1974 [12], there have been a large number of SAs for the development of giant and ultrashort pulsed lasers. There were reports on some man-made devices such as semiconductor saturable absorber mirrors (SESAM) or few materials that have great optical and electrical properties. SESAM is made up of multiple semiconductor material layers that were produced via atomic layer deposition or other microfabrication technologies, and these layers often contain a reflective mirror for the free-space alignment of a fibre laser cavity [12]. As a result, SESAM's two main weaknesses are the difficulty in manufacturing and the integration of an all-fibre laser cavity. Additionally, its broad applications are limited by inadequate beam quality, a minimal threshold of damage, and a limited operating bandwidth contained within 10 nm [13]. These devices use the nonlinear polarisation rotation [14] approach and nonlinear optical loop mirrors (NOLM) [15]. Two-dimensional (2D) materials have gained a lot of attention later in the realm of passive giant and ultrashort laser pulse production as excellent possibilities for SAs. The passively Q-switched and mode-locked fibre lasers established on 2D materials exhibit the nonlinear ultrafast photoelectric reaction of those 2D materials.

Retrospectively, Set *et al*., [16] made the initial proposal for carbon nanotube (CNT) SAs for a passively mode-locked laser back in 2004. With many benefits such as superior nonlinear optics (NLO) exposures, low diffusion intensity, quick recovery time as well as sub-picosecond relaxation time, CNT overcomes the shortcomings of SESAM. However, the CNT's integration in longer working wavelengths, for example 2 μm, is constrained by the challenges in chirality and tube diameter management [17]. Afterwards, Hasan *et al*., [18] and Bao *et al*., [19] made the first demonstration of graphene SA in 2009. Despite having an intrinsic zero bandgap for operating in the visible, near, and mid-infrared ranges, graphene's smaller on/off ratio of switching and low absorption of 2.3 % for each layer limit its laser output capability and useful optoelectronics applications [20]. Through

adaptable defect engineering, transition metal dichalcogenides (TMD) were shown to have scalable bandgap properties after graphene [21].

TMD has both semiconductor and superconducting properties, the ability to switch from an indirect bandgap to a direct bandgap, nonlinear absorption properties, and increasing modulation depth with decreasing thickness [22]. Yet only monolayer TMD commonly exhibits the direct bandgap feature, which necessitates a challenging synthesis and defect engineering technique [23]. By switching from an indirect to a direct bandgap, these mono-elemental materials can adjust their bandgap and other features [24]. However, they still face the problem of oxidative instability [25].

Gogotsi *et al*., [26] originally found the MAX phase in 2011 in order to demonstrate 2D Ti3C2 nanosheets, multi-layer structures, and conical scrolls in addition to the aforementioned SA materials, thus increasing research interest in this material in a variety of fields, including actuators [27], sensors [28], clean water generation [29], photothermal treatment [30], and lithium-sulphur batteries [31]. Due to their exceptional features, 2D transition metal carbides, carbonitrides and nitrides have recently received a lot of interest [32, 33]. These MAX phases or MXene was proven to display higher nonlinear saturable absorption due to strong electrical conductivity as well as extremely adaptable electro-optical characteristics [34-37]. Based on MXene Ti3C2Tx-PVA film SA, stable mode-locked pulsations are effectively produced in a fibre laser [33, 35].

MAX phases, the antecedent of MXene, sparked intense curiosity in response to MXene. The broad formula for MAX phases is Mn+1AXn, where M is a transition metal (Sc, Ti, Hf, Zr, Nb, V, Ta, Cr, Mo, etc.), X is carbon or nitrogen or a combination with n = 1, 2, and 3, and A represents group III, IV, V, or VI element (Al, Ga, P, As, S, In, Si, Ge, Sn, , etc.), giving it a unique atomic arrangement structure [38, 39]. These sorts of substances give MAX phase materials the dual qualities of metal and ceramic, such as good oxidation resistance, elevated temperature resistance, and elevated temperature flexibility like ceramic and metal, respectively [40, 41]. The latter two characteristics are advantageous for producing ultra-short laser pulses. Furthermore, delamination makes it possible to create mono-layer MXene of a thickness of less than 1 nm and lateral diameters on the order of m [52]. Recently, passively Q-switched, and mode-locked fibre lasers have successfully used MAX phase Ti3AlC2 as SA [42, 43]. Following careful examination of the MAX phase materials in the system of Ti-Al-C, Ti2AlC was identified due to its distinctive characteristics.

By incorporating MAX phase Ti3AlC2 as the SA in any erbium-doped fibre laser (EDFL), Ahmad *et al*., [44] accomplished the Q-switched pulse train in 2020. This was made possible by exceptional optical and electrical assets of Ti3AlC2 Following that, MAX phase materials such as V2AlC, Ti3CNTx, Nb2CTx, Ta4C3Al have been widely synthesised and fabricated as SAs using various methods and techniques for showing pulsed laser operations, by employing passive Q-switching as well as passive mode-locking [45-49].

This review studies the synthesising, fabricating, and incorporating techniques of MAX phase materials due to their distinctive features, with special attention given to Ti-Al-C combinations as a successful example. Hitherto, the utmost stable material in the Ti-Al-C regime is Ti2AlC [50]. Since Ti2AlC has a lower Fermi level than Ti3AlC2, it is simpler to achieve an electrical transition between bands. Additionally, MAX phase materials have a higher optical conductivity than anticipated for optimum photoelectric response [51]. Al particles react together with oxygen in the air to form a strange oxide coating that stops the material from further oxidising, giving the Ti2AlC a higher amount of Al atoms than Ti3AlC2 and a higher antioxygenic characteristic [52]. Due to these benefits, MAX phase materials are more environmentally stable and facilitate the generation of Q-switched laser pulses. While MXene may seem to be a more recent material than graphene, TMD, black phosphorus, and other materials, it has already begun to get scientific attention as a strong SA contender.

The recent innovation by MAX phases and MXene SA to produce Q-switched fibre lasers in the near- and mid-infrared frequency band will be the main focus of this study. The studies are anticipated to provide readers with more information about the investigation of MXene-based SAs in passively Q-switched fibre lasers. These studies may also inspire further research in light of numerous demonstrations, problems, and challenges, as well as the broader implications that these studies have brought about.

Much effort has been made on MAX phases and MXene synthesis and production in order to enhance pulse laser properties, notably with the all-fibre laser configuration and the influence of SA integration techniques into the laser cavity. The present state-of-the-art synthesis, fabrication, and inclusion of MAX phase or MXene SAs in all-fibre laser cavity architecture is the topic of this review study.

2. MXene and Max-Phase Synthesisation and Fabrication

MXene molecule, which takes on several chemical forms based on the periodic table's M, X, and T elements, is created when the surface terminal group element in a MAX phase compound is exfoliated. The majority of MXene synthesis to date has been done top-down, particularly with regard to the selective etching of their MAX phases [53]. The synthesis and fabrication of MAX phases and MXene as listed in **Error! Reference source not found.** including Ta_4C_3Al, $Ti_3C_2T_x$, Ti_3CNT_x, Ti_2CT_x and Nb_2CT_x as SAs are reviewed in this section.

Table 1
Synthesisation techniques of MAX phases and MXene

Synthesisation and fabrication
Aqueous acid etching method (AAE)
Electrochemical exfoliation (ECE)
Two-step exfoliation scheme
Dispersion via AAE method (D-AAE)
Stirring and ultrasonic vibration (USV)
Liquid phase exfoliation method
Solution-casting method (SCM)
Fusion of polyvinyl alcohol with MAX phase
Aqueous acid etching method (AAE)

2.1 Aqueous Acid Etching Method

MXene molecule, the Ti_3AlC_2 powder was combined for 48 hours at room temperature with 40 wt.% hydrofluoric acid (HF), washed many times with DI water, and the resultant deposition was let to dry in a vacuum-oven for 48 hours at 60 °C [54]. $Ti_3C_2T_x$ MXene can also be replaced by MAX phase Ti_3AlC_2 in the final product. However, aqueous acid etching methods can be used as references to develop $Ti_3C_2T_x$. In Naguib's study [43], Ti_2AlC was employed as raw materials, and then ball-milled and heated up to 1350 °C for two hours under argon gas conditions. The powder was then exposed to 40 wt.% HF at a volume ratio of 1:10 at room temperature for two hours. The obtained deposit was centrifuged to separate the particles and cleansed with DI water.

Using a volume ratio of 1:15, Ti_3AlC_2 solution and 40 wt.% HF were combined to perform an aqueous acid etching procedure [55]. The deposit was cleansed with DI water to achieve a pH of more than 6, and then dried in a vacuum oven. After diffusing the powder-formed $Ti_3C_2T_x$ in IPA below 20

°C temperature for 10 hours, the $Ti_3C_2T_x$ was subjected to water bath sonication to exfoliate the material. The liquid suspension was then centrifuged for 30 minutes at 3000 rpm, followed by another 30 minutes at 18000 rpm for the supernatant. To create a suspension of $Ti_3C_2T_x$, the precipitate was mixed with DI water after the supernatant was removed.

Additionally, Ti_2AlC MXene has recently been shown to perform better than Ti_3AlC_2 in a number of areas, including stability [56], electronic band transition [57], optical conductivity [58], and oxidation resistance [59]. However, this Ti_2AlC was produced directly from the commercially available product without the need for synthesis [57]. Polyvinyl alcohol (PVA) was used to create a composite out of Ti_2AlC in a 1:1 ratio. The characterisation of this Ti_2AlC was carefully studied using several techniques, including the XRD, EDS, and Raman spectra, SEM images, and absorption spectra.

Another work presented further aqueous acid etching method for the synthesis of $Ti_3C_2T_x$ solution of nanosheets. The deposit was firstly dried up using a vacuum oven before the $Ti_3C_2T_x$ powder was dispersed in N-methyl-2-pyrrolidone at a dilution of 1 mg/ml. (NMP) [60]. To get the $Ti_3C_2T_x$ nanosheet solution, the supernatant was then centrifugated at 4000 rpm at 10 °C for 20 minutes. In another research work [61], a similar synthesis technique was also reported.

On the other hand, the energy of formation of V2C from the fresh material, V_2AlC, at 2.981 eV, is regarded low compared to other MXene in the M2X system, which may make it challenging to synthesise extremely pure V_2CT_x [62]. As a result, obtaining delaminated flakes is difficult since V_2CT_x does not have a precise crystalline structure [63]. The original V_2AlC phase was etched in HF and intercalated with tetrabutylammonium hydroxide (TBAOH) to create the V_2CT_x using aqueous acid etching technique [64]. The mixture was sonicated in DI water after the excess TBAOH had been removed, creating the colloidal suspension. The suspension was then spin cast to create a 400 nm thick V_2CT_x film. The flakes exhibit exceptional quality, softness, foldable and overlapped in several places. Based on the UV-VIS-NIR transmittance curve, the V_2CT_x exhibits a wide absorption spectrum, especially for thinner V_2CT_x films like those with a thickness dimension of 10 nm, spanning the wavelength range of 500 to 2700 nm without any discernible transition.

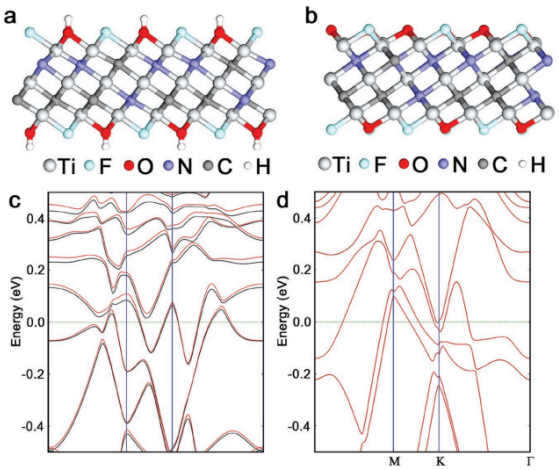

Fig. 1. Monolayer Ti_3CNT_x - schematic structures with (a) fluorine and hydrogen groups and (b) fluorine and oxygen groups, (c)-(d) the corresponding structures of electronic band, J. Li *et al*., [66]

Ti_3CNT_x's physical characteristics are comparable to those of $Ti_3C_2T_x$ [65]. Different surface terminations were shown in the monolayer Ti_3CNT_x schematic structure as given in [66]. Ti_3CNT_x was created by substituting a nitrogen atom for one of the four carbon atoms to create a mix arrangement

of C and N. In comparison to other semiconducting 2D materials, monolayer Ti_3CNT_x exhibits more prominent metallic properties as a result. In contrast to Van der Waal's attraction, the hydrogen bond is principally responsible for the stacking of monolayer Ti_3CNT_x. Indirect hydrogen connections are formed by intercalated water molecules or surface functional groups to form these hydrogen bonds [67]. As with monolayer Ti_3CNT_x, the electrical band structures of layered Ti_3CNT_x are retained. This indicates that a successful SA is possible without a demanding technique to produce a monolayer solution.

By employing 30% HF solution to etch the Al layers from the Ti_3AlC_2 raw material, an alternative MXene, Ti_3CNT_x was created [66]. First, 20 ml of 30% aqueous HF solution was combined with 2 g of Ti_3CNT_x powder at ambient temperature. The mixture then was agitated for 18 hours employing a magnetic bar. The mixture was then centrifuged at a speed of 3500 rpm for 3 minutes after being washed with DI water, mixed for 1 minute, and dried. This procedure was done five times, and then the supernatant was decanted until its pH level was more than 6. The multi-layered Ti_3CNT_x was then delaminated by combining the Ti_3CNT_x sediment with an aqueous mixture of 55% TBA-OH at a ratio of 100:1. After that, the mixture was stirred at ambient temperature for 4 hours. The mix was then centrifuged for 2 minutes at 3500 rpm, and the supernatant was then decanted. To further disseminate the particles, DI water was added after which the sediment was centrifuged and the remaining TBAOH was removed by transferring the supernatant three times. Then the residue was given 100 ml of DI water. After being sonicated for nearly one hour, the mixture was centrifuged at the revolution of 3500 rpm for an additional hour. Finally, the mono- to few-layer Ti_3CNT_x supernatant was created. Both the monolayer Ti_3CNT_x and their stacked systems' optical absorption coefficients, which range in wavelength from 1000 to 3500 nm, were computed.

Another illustration of how to make V_2CT_x powder is as given in [67] by using the standard aqueous acid etching procedure [68]. First, for 48 hours at 35 °C, the V2C powder was constantly mixed in a solution of 2 g of 200 mesh V_2AlC and 40 ml HF acid. The mixture was then diluted with DI water, and centrifugation was performed numerous times at 5000 rpm for 10 minutes per cycle, till the pH value of the supernatant surpasses 6. The carved V_2AlC was accrued using a PVDF membrane (mesh of 0.450) for filtering, and it was then cleansed with 2 litres of DI water. Then, using a 400 W built-in water-cooling system and a constant temperature of 10 °C for 30 minutes, bath sonication was used to separate the layers (delaminate) the V_2AlC. The dispersion was then centrifuged for 30 minutes at 5000 rpm to extract the V_2CT_x nanosheet supernatant. To get the precipitate, the supernatant was centrifuged once more at 18,000 rpm for 30 minutes. This precipitate was maintained under vacuum for 24 hours at 80 °C.

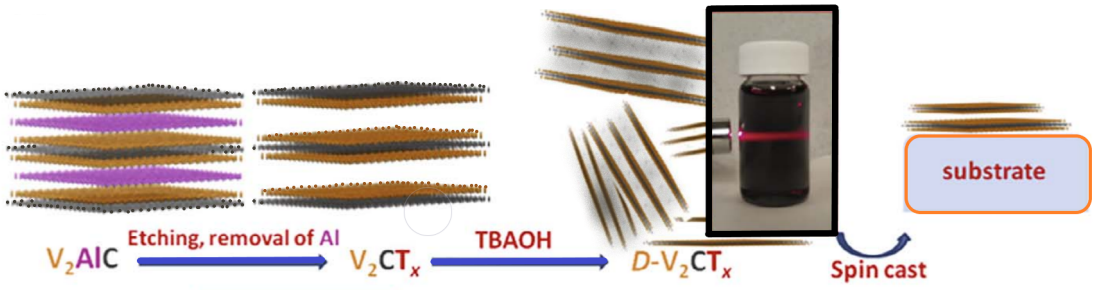

Fig. 2. Schematic diagram to prepare V_2CT_x to spin-cast the V_2CT_x film [106]

Nb_2C research began in 2013, when Naguib *et al.*, [69] synthesised the Nb_2AlC successfully. The acquired linear absorption spectra have been used to compute the optical bandgap of Nb_2C, which is determined as 0.81 eV [70]. The approximate intensities of anomalous phonon-phonon scattering

and scattering of electron-phonon cause a substantial decrease in the thermal conductivity of the lattice in Nb_2C [71]. In the near-IR region, Nb_2C has been shown to have a high photothermal conversion efficiency and substantial absorption [72].

By treating Nb_2AlC with a 50% HF mixture at ambient temperature, the Nb_2C was produced using an acid etching technique [73]. After the etching, the surplus HF was periodically washed together with DI water and centrifuged until the pH was more than 6 at a speed of 3000 rpm. The Nb_2C suspension was then collected using a cellulose membrane following filtering. The as-produced multilayer Nb_2C was then thoroughly mixed for 3 days at room temperature in 30 ml of 25% tetra-propylammonium hydroxide (TPAOH) solution. The TPAOH was then eliminated by centrifuging the mixture at 15,000 rpm for 10 minutes after rinsing it with DI water. Following a redispersion in ethanol and dimethylformamide (DMF), the precipitate was centrifuged at 3000 rpm for 10 minutes to split colloidal from un-delaminated Nb_2C flakes. Finally, a few-layered Nb_2C nanosheet was created, and must be stored at 5 °C to increase its longevity.

2.2 Electrochemical exfoliation

It is anticipated that the MAX phases would have improved stability and superior qualities due to termination of the functional groups on its surface [74]. However, the addition of HF to the AAE procedure results in the synthesis of MAX phases or MXene that has oxygenic as well as hydrophilic termination groups, mainly, -O and -OH, on its surface, reducing its material characteristics and environmental stability [75].

Aqueous HF etching is commonly used to exfoliate stacked MAX phases; however, HF is a very acidic solvent that can seriously contaminate surfaces and leave them with flaws [76]. This safety concern may be resolved by using a much safer and simpler electrochemical exfoliation-based synthesis method, for example, one that uses a highly fluorinated nonaqueous ionic liquid as the electrolyte to create $Ti_3C_2T_x$ quantum dots (QDs) with improved constancy [112]. As shown in FIGURE 3 below, a three-electrode electrometrical system is used to build the synthesis tool. This system consists of a working electrode (bulk Ti_3AlC_2), an electrode of quasi-reference (Ag), and a counter-electrode (Pt).

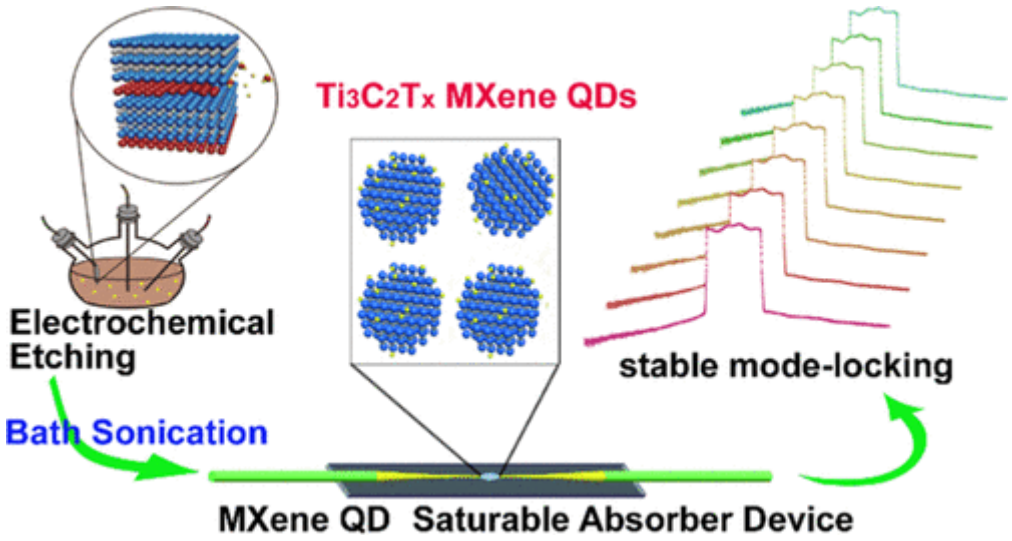

Fig. 3. Synthesis setup of $Ti_3C_2T_x$, F. Yang *et al.*, [111].

In order to make the nonaqueous electrolyte, 20 g of [EMIM][PF_6] was combined with 100 ml of MeCN. Then, a 150 ml container made up of three electrodes and a glass tubing, was filled with the combined solution. The combined solution was then used after being bubbled with argon gas for 5 minutes. The Ag wire would receive a continuous potential of 3 – 7 V in a procedure lasting for 5 hours. The $PF6^-$ was then electrolytically decomposed into F^- while the Al layer was being removed from the Ti_3AlC_2 by selective etching. Then, the electrolyte was observed to turn brown in colour and contain shards of $Ti_3C_2T_x$ and powder. Following that, two centrifugation operations were performed in fast succession; the first at 3500 rpm for 30 minutes to remove big elements from the electrolyte and the second for 30 minutes at 7000 rpm to collect the sediment. Afterwards, silts were added to the MeCN and ultrasonically treated for 10 hours at atmospheric N2 gas pressure. The $Ti_3C_2T_x$ QD was then produced by centrifuging the supernatant for 30 minutes at 7000 rpm to eliminate the contaminants of certain large particles.

2.3 Two-step exfoliation scheme (Ta_4C_3)

A two-step exfoliation approach as illustrated in figure 4 was used to produce nanostructured Ta4C3 nanosheets, resulting in nanosized 2D Ta_4C_3 MXene ultrathin nanosheets. Due to the increased manufacturing complexity for outstanding 2D topology, there were less investigations on 2D Ta_4C_3 nanosheets compared to other MXenes. First, the bulk MAX-phase Ta_4AlC_3 ceramics were sintered for 2 hours at 1500 °C using a solid-phase sintering process. The sandwiched aluminium layer between Ta_4C_3 MXene layers was etched for four days at room temperature in 40% hydrofluoric acid (HF) aqueous solution. The delaminated Ta_4C_3 MXene was then ultrasonically shaken in deionized water (DI) for 15 hours. The solution was then centrifuged at 10,000 rpm for 10 minutes to obtain the supernatant liquid [49].

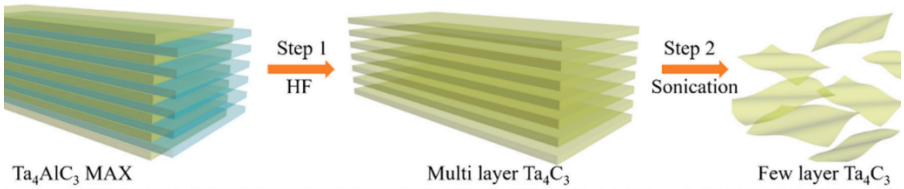

Fig. 4. Preparation route of few-layer Ta4C3 MXene using two-step exfoliation [66]

2.4 Dispersion via the aqueous acid etching method.

Aqueous acid etching has been used in various research papers to explain how to create $Ti_3C_2T_x$ dispersion. The MAX phase Ti_3AlC_2 was immersed in 40% HF and agitated at 500 rpm for 20 hours at room temperature to create the $Ti_3C_2T_x$ flakes [77]. Once the pH was more than 6, the bulk $Ti_3C_2T_x$ solution was collected and cleansed with DI water. After 24 hours of probe-ultrasonication using a cell grinder, the $Ti_3C_2T_x$ flakes were obtained. $Ti_3C_2T_x$ suspension preparation likewise utilised HF etching with isopropanol as the solvent, and liquid phase exfoliation (LPE) was used to create the thin film [78].

2.5 Stirring and ultrasonic vibration.

Stirring and ultrasonic vibration (USV) could also be used for a straightforward synthesis method of $Ti_3C_2T_x$ solution [79]. First, a beaker containing 40 ml of 0.008 g/ml PVA solution and 10 mg of

Ti_3AlC_2 powder was agitated for 24 hours. The agglomerated Ti_3AlC_2 was then broken apart by cavitation using ultrasonication for 2 hours. The last step in the synthesis of $Ti_3C_2T_x$ solution was to separate the supernatant from the solid residue.

2.6 Liquid Phase Exfoliation (LPE) method.

The LPE approach could be used to create $Ti_3C_2T_x$ nanosheets in addition to USV [80]. First, a water bath at a temperature below 20 °C was used to dissolve 20 mg powder of $Ti_3C_2T_x$ into a solution of 20 ml of ethanol. After that, this dispersion was subjected to ultrasonic treatment utilising 200 W of power for 12 hours. After centrifuging the $Ti_3C_2T_x$ solution for 30 minutes at 3000 rpm to remove big bulks, the $Ti_3C_2T_x$ nanosheet supernatant was produced. Additionally, the LPE approach may also be used to create Nb_2C nanosheets [81, 82]. First, 10 ml of IPA solution was used to dissolve 50 mg of Nb_2C powder. The mixture was then sonicated for 4 hours at 40% power. The homogenous Nb_2C nanosheet in IPA solution was then obtained by centrifuging the suspension for 10 minutes at 4000 rpm to remove any undissolved flakes.

In another study, a few-layer Ta4C3 MXene was produced using the LPE method. To remove the Al layers, the bulk Ta_4AlC_3 was immersed in 40% HF aqueous solution for two days at 30 °C. After etching, the mixture was repeatedly washed with DI to neutralise it. Then, the mixture was centrifuged at 5000 rpm for 30 minutes to recover the multi-layer Ta_4C_3. Then, using an ultrasonic probe with a power of 500 W, the created multi-layer Ta_4C_3 was re-dispersed in N-methyl pyrrolidone (NMP) solution and sonicated for 8 hours at 5 °C. To get the few-layer Ta_4C_3, the product was centrifuged between 5000 and 8000 rpm [111].

2.7 Solution-casting method

The Ti_3AlC_2 powder was first etched with 50 wt.% HF at room temperature for 6 hours. Vacuum-aided filtering was used to capture the $Ti_3C_2T_x$ residue using a polyvinyl difluoride filter (PVDF) membrane. $Ti_3C_2T_x$'s clay structure was dried up in a vacuum oven for 24 hours at 80 °C. The thin-film structure of the SA device was created using a solution-casting technique with PVA and Ti3C2Tx powder (PVA). First, a beaker containing 40 ml of deionized (DI) water, 40 mg of PVA powder, and 20 mg of $Ti_3C_2T_x$ powder was swirled for 24 hours at room temperature. The resultant solution was then subjected to a 2-hour ultrasonication to disperse the $Ti_3C_2T_x$ particle agglomeration. Finally, the solution was applied to the D-shaped fibre as an SA device. A 5 ml portion of the prepared solution was set aside and allowed to dry for 48 hours in a clean petri dish. The thin dried layer was afterwards removed from the petri dish [92].

2.8 Polyvinyl alcohol fusion with MAX Phase

Due to its good film-forming capabilities, superior tensile strength, ease of emulsification, and superior water solubility, PVA has been shown to be a reliable host polymer for thin film fabrication. PVA is a better host material because it can endure powerful laser light within the cavity; thanks to its high melting point of 200 °C, which is higher than that of polymethyl methacrylate (PMMA) with a melting point of 160 °C, and polyethylene oxide with a melting point of 67 °C. Deionized (DI) water was used to dissolve the PVA solution's powder. An electronic balance was used to weigh 1 g of PVA powder, which was then combined with 120 ml of DI water in a beaker. The mixture was put on a hot plate and agitated for 45 minutes at 200 °C and 300 rpm. The next step was to combine the produced PVA solution with Ti_3AlC_2 powder to create a free-standing thin film SA. A few Ti_3AlC_2 powders were

first placed on an electronic scale so they could be weighed. Then, 40 ml of PVA solution were combined with 10 mg of Ti_3AlC_2 powder. The mixture was magnetically swirled for 24 hours at room temperature on a hot plate. The combination was further subjected to ultrasonication for 2 hours at the same temperature. The Ti_3AlC_2 solution residue visible on the surface of the supernatant indicated that the sonication procedure was effective. A tidy petri dish was filled with 5 ml solution of Ti_3AlC_2-PVA and was left out in the open for 48 hours. Peeled off the petri dish was the dried 3-cm diameter MAX-PVA thin film with a thickness of 30 m [38].

3. MXene and Max-Phase Synthesisation and Fabrication

The initial but most crucial step in this laboratory circuit level experiment—in setting up the laser cavity—is the inclusion of the manufactured MXene or MAX phase SA made from bulk MAX phase powder. There are several methods for creating the SA thin films that can go within the all-fibre cavity laser such as tapered fibres, D-shaped fibres, etched fibres, and flat-faced fibre ferrules.

Table 2
SA incorporation techniques applied with MAX phases and MXene

Fibre preparation	SA incorporation
Tapered fibre	Optical deposition
	Spraying
	Magnetron sputtering deposition
D-shaped fibre	Drop-casting
	Dripping
	Monolayer film
	Evanescent coupling
Etched fibre	Inkjet printing
	Syringe injection
	Immersion and optical deposition
Fibre ferrules	PVA composite film

3.1 Tapered fibre

By progressively stretching an optical fibre while it is heated, for example, over a flame, until the glass softens, one can create a tapered optical fibre. With this technique, the fibre is thinned over a small area, perhaps a few centimetres or millimetres. The core of the fibre thins out by the same percentage as the entire fibre. A common process for creating tapered fibres is flame-brushing [81]. By melting the optical fibre using an oxy-LPG flame and drawing it through a translational step to lower its waist diameter, the flame brushing process is typically used to create tapered fibres [83]. For the interaction of absorbing materials with high heat dissipation mechanisms, the tapered fibre creates an evanescent field around its waist area [84].

3.1.1 Optical deposition to tapered fibre

On the tapered fibre platform, the SA can be created using a variety of techniques. The most frequent technology used to fabricate SAs is optical deposition. For instance, a H_i-1060 fibre has a 5.2-µm waist diameter and a 3-mm waist length [25]. The V_2CT_x nanosheets were deposited utilising the optical deposition approach employing a 980-nm pump on the waist section of the tapered fibre,

where material adsorption becomes apparent because of evanescent contact. The entire procedure was detected using a power meter. An oxy-hydrogen flame was used in the second tapering configuration for SMF-28, and the tapering resulted in a 13-µm waist diameter [86].

A comparable optical deposition was used with droplet volumes of 5 – 10 l and a 60 mW light source [86]. When the optical loss reached 3 dB, the deposition was terminated. A further tapered fibre with 9.21 m waist diameter and an insertion loss of 0.69 dB was used for optical deposition of a Ti3C2Tx solution using a 980 nm laser pump and a power meter [86]. The deposition was along the 200 µm length and the insertion loss is 1.39 dB. Under real-time monitoring, a tapered fibre with a waist diameter of 12 µm and a waist length of 5 mm was also optically deposited with Nb_2C SA [22].

It took around 3 minutes to conclude the deposition. Another illustration is a tapered fibre using a $Ti_3C_2T_x$ SA optical deposition process that has a 15 µm waist diameter [77]. To ensure that the proper amount of $Ti_3C_2T_x$ sample was injected on the tapered fibre, the optical deposition of $Ti_3C_2T_x$ SA was conducted with a needle tube [87].

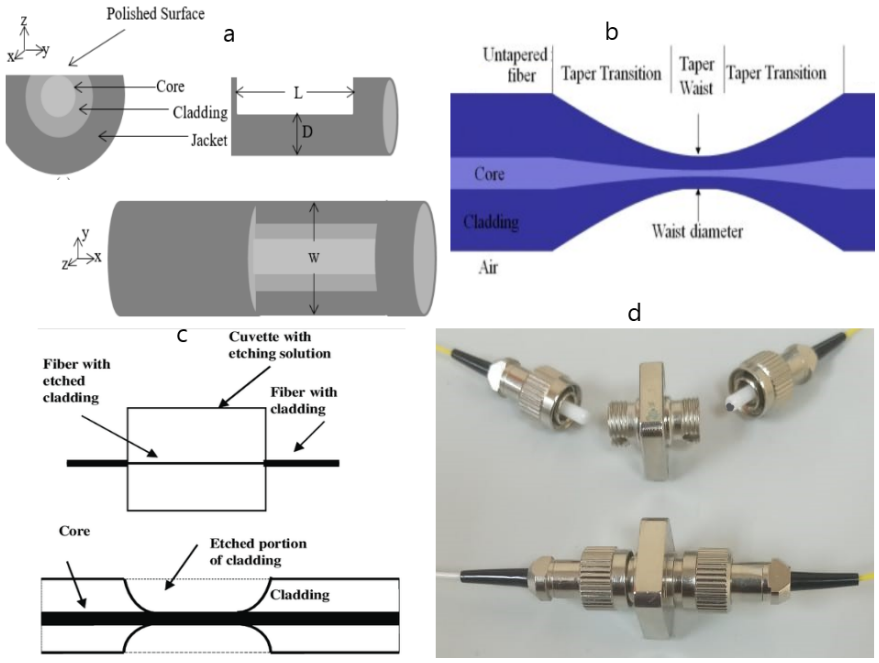

Fig. 5. Incorporation of SA. a) D-shaped fibre b) tapered fibre c) etched fibre d) fibre ferrule [47]

3.1.2 Spraying and magnetron sputtering deposition to tapered fibre

The Nb_2C suspension was sprayed over a 3.56 µm diameter tapered fibre platform's waist region, which was placed on a 60 °C hot plate, evaporating the solvent as soon as it made contact with the hot plate, creating the SA [88]. The optical loss is calculated as 1.55 dB. Additionally, employing magnetron sputtering deposition (MSD), a few-layer Nb_2C N Nb_2C nanosheet was deposited on the tapered fibre [89, 90]. In order to increase film adhesion on the surface of fluorine mica (FM), FM was first hydrophilically treated with concentrated HF and H_2SO_4. After that, alcohol and DI water were used several times to clean the FM sheet. After treatment, an oven was used to dry the FM sheet. Then, a 40 °C oven was used to dry the treated FM sheet. The targets for FM and MXene were then installed within a magnetron sputtering chamber setup. A vacuum of $6.8x10^{-4}$ pa was created within the chamber using mechanical and atomic pumps. Finally, a consistent MXene film was

created by spinning the FM at 30 rpm. The MXene film was then sputtered on a microfibre substrate with a waist diameter of 18.03 µm using the same pressure and rotation speed.

3.2 D-shaped fibre

D-shaped fibre, also known as a D-type optical fibre has its cladding side polished, giving it a D-shaped appearance. There are several applications for D-shaped optical fibres, particularly in sensing. A metal and dielectric system have established a surface plasmon wave dispersion relationship. Another form of microfiber that causes evanescent contact with absorbent materials on its polished surface is also the D-shaped fibre [90]. Compared to the tapered fibre structure, the side-polished fibre structure is extra robust [91].

A higher nonlinear interaction length, a higher value of optical damage threshold, and a significantly increased interaction of light-matter are only a few further benefits of the D-shaped fibre [92, 93].

3.2.1 Drop-casting to D-shaped fibre

Another work provides a detailed mechanically based fabrication process for D-shaped fibres, which was used to drop-cast a $Ti_3C_2T_x$ solution to generate the SA, with a 71.69-µm fibre diameter, 4.69-µm core-cladding space, and 1400-µm polishing length [94].

3.2.2 Dripping and monolayer film to D-shaped fibre

For the ultrasonic dripping of Ti3C2 nanosheet dispersed with 0.1 mg NMP, an additional D-shaped fibre with 6-µm polishing depth from the centre was used [95]. Insertion loss and polarisation determined loss (PDL) of a stacked Ti_3CNT_x monolayer film connected to a D-shaped fibre at 1557 nm were 4.5 dB and 1.8 dB, respectively [96]. The transverse magnetic (TM) and transverse electric (TE) modes' optical signal-to-noise ratios alter according to the PDL, which is a measurement of distribution of peak-to-peak optical power by all polarisation states [97]. As a result, the TE and TM modes significantly affect how the laser beam's saturation level is modulated, changing the depth of a SA's modulation evanescent coupling to the D-shaped fibre.

3.2.3 Inkjet printing to D-shaped fibre

Additionally, a D-shaped fibre with 6 µm side-to-core depth was used to conduct the evanescent-coupling of Ti_3C_2Tx solution containing 6.67 mg/ml [98]. At 1900 nm, the insertion loss was 2.0 dB and the PDL was 5.2 dB. Inkjet printing is used to make use of the benefits of 2D materials for printed optoelectronic devices, including their tiny footprint, simplicity of integration, geometric compatibility, scalability as well as cost factor [99]. A D-shaped SA was created by imprinting a homogeneous, continuous Ti_3C_2Tx nanosheet film with a 35-m inter-droplet spacing on the D-shaped fibre.

3.3 Etched fibre

The optical fibre was submerged in a 30% HF acid solution for 2 hours to produce an etched fibre in addition to polishing the D-shaped fibre using the aforementioned mechanical method [100]. The coating on the silica glass component was removed by HF.

3.3.1 Syringe injected to etched fibre

The residual HF solution was rinsed from the surface of the etched fibre using clean water and ethanol. The etched fibre was placed in a protective jacket, and $Ti_3C_2T_x$ solution was injected with a syringe. The liquid $Ti_3C_2T_x$ within the protective sleeve was sealed by melting the ends of the sleeve with a hot iron and bonding them together with glue. Due to its geometrical symmetry, which is more robust than that of the D-shaped fibre, this SA structure helps to increase the thermal damage threshold brought on by physical contact [101]. However, compared to its application in a range of sensors such biosensors [102], refractometric sensors [103], and humidity sensors [104], the employment of an etched fibre platform as an SA is less frequent. This is because its nanometer-sized fibre ends—the primary end product of etched optical fibre—are difficult to produce using either tapering or mechanical polishing methods [105]. Etched fibre manufacturing is more dangerous than D-fibre production due to the integration of HF and should not be handled continuously, even while wearing appropriate protection gear.

3.3.2 Immersion and optical deposition of etched fibre

Another study involved dipping the etched fibre in Ti3C2 solution to create SA [106]. By using optical deposition using a laser light source, the Ti3C2 solution was drawn to the surface of the cut fibre.

3.4 PVA composite film in fibre ferrules

The simple and slightly easier method is to construct the SA by sandwiching an absorbent material such as $Ti_3C_2T_x$ between two fibre ferrules while manufacturing either the MXene or the MAX phase into a thin film [107]. A $Ti_3C_2T_x$ composite film was generated by combining 10 ml of $Ti_3C_2T_x$ with PVA solution of 10 ml that had been exposed to a 24-hour ultrasonic treatment. A 1-mm^2 piece of $Ti_3C_2T_x$/PVA composite film was inserted between two fibre ferrules to make the SA. The fibre ferrule structure is easier to manage and operate than microfibers due to material contact between the absorbent and the fibre ferrules. Nevertheless, it has a briefer length of interaction and lesser threshold of optical damage [108].

Table 1
Summary of MAX phase and MXene saturable absorber synthesis, fabrication, and incorporation.

Research Period		LASER Configuration			Incorporation of Saturable Absorber			
Research No.	**YYYY-MM**	**Pulse Regime**	**Cavity**	**MAX Phase / MXene**	**Synthesisation**	**Fabrication or Deposition**	**Incorporation**	**Ref.**
1	2022-02	M-L	EDFL-AF-Ring	Ta_4C_3Al	LPE	Drop Casting	Fibre ferrule	[111]
2	2021-12	Q-S	EDFL-AF-Ring	Ta_4C_3Al	Two-step exfoliation	Laser deposition	Fibre patch cord	[49]
		M-L	EDFL-AF-Ring	Ta_4C_3Al	Two-step exfoliation	Spin Coating	Fibre patch cord	
3	2021-11	M-L	TDFL-AF-Ring	Nb_2CT_x	LPE	Microfiber Coat	Tapered fibre	[82]
		M-L	THDFL-AF-Ring	Nb_2CT_x	LPE	Spin Coating	Tapered fibre	
4	2021-08	M-L	THDFL-AF-Ring	$Ti_3C_2T_x$	ACE	Dripping	D-shape fibre	[95]
5	2021-06	Q-S	EDFL-AF-Ring	Ti_2CT_x	SCM	Solution Casting	Fibre ferrule	[57]
		M-L	EDFL-AF-Ring	Ti_2CT_x	SCM	Solution Casting	Fibre ferrule	
6	2021-04	Q-S	BDFL-AF-Ring	Nb_2CT_x	SCM	Solution Casting	Fibre ferrule	[47]
7	2021-03	M-L	THDFL-AF-Ring	$Ti_3C_2T_x$	ACE	Drop Casting	D-shape fibre	[98]
8	2021-02	Q-S	HDFL-AF-Ring	Nb_2CT_x	SCM	Solution Casting	Fibre ferrule	[46]
9	2021-01	M-L	TDFL-AF-Ring	Nb_2CT_x	ACE	Optical Deposition	Tapered fibre	[56]
11	2021-01	M-L	EDFL-AF-Ring	Nb_2CT_x	LPE	Spray & Evaporate	Tapered fibre	[84]
12	2020-11	M-L	EDFL-AF-Ring	$Ti_3C_2T_x$	SCM	Drop Casting	Fibre ferrule	[36]
		M-L	EDFL-AF-Ring	$Ti_3C_2T_x$	SCM	Solution Casting	Fibre ferrule	
13	2020-11	M-L	EDFL-AF-Ring	Nb_2CT_x	-	Sputtering deposit	Tapered fibre	[92]
14	2020-11	M-L	YDFL-AF-Ring	$Ti_3C_2T_x$	EC Exfoliation	Optical Deposition	Tapered fibre	[78]
15	2020-10	M-L	EDFL-AF-Ring	$Ti_3C_2T_x$	Stirring and USV	Drop Casting	Fibre ferrule	[42]
16	2020-07	M-L	EDFL-AF-Ring	$Ti_3C_2T_x$	PVA Fusion	Solution Casting	Fibre ferrule	[38]
Research Period		**LASER Configuration**			**Incorporation of Saturable Absorber**			

Research No.	YYYY-MM	Pulse Regime	Cavity	MAX Phase / MXene	Synthesisation	Fabrication or Deposition	Incorporation	Ref.
17	2020-04	Q-S	EDFL-AF-Ring	$Ti_3C_2T_x$	SCM	Solution Casting	Fibre ferrule	[45]
18	2020-12	M-L	EDFL-AF-Ring	$Ti_3C_2T_x$	LPE	Solution Casting	Fibre ferrule	[83]
		M-L	EDFL-AF-Ring	$Ti_3C_2T_x$	LPE	Film Attached	Fibre ferrule	
19	2020-07	M-L	EDFL-AF-Ring	$Ti_3C_2T_x$	ACE	Optical Deposition	Tapered fibre	[90]
20	2020-07	Q-S	TBFL-AF-Ring	$Ti_3C_2T_x$	LPE	Microfiber Coat	Tapered fibre	[44]
21	2020-03	M-L	YDFL-AF-Ring	NPE	ACE	Optical Deposition	Tapered fibre	[68]
		M-L	YDFL-AF-Ring	V_2AlC	ACE	Optical Deposition	Tapered fibre	
		HM-L	YDFL-AF-Ring	NPE- V_2AlC	ACE	Optical Deposition	Tapered fibre	
22	2020-03	M-L	-	$Ti_3C_2T_x$	ACE	Optical Deposition	Tapered fibre	[77]
23	2020-01	M-L	-	$Ti_3C_2T_x$	ACE	Optical Deposition	Tapered fibre	[78]
24	2019-04	M-L	EDFL-AF-Ring	$Ti_3C_2T_x$	ACE	Optical Deposition	Tapered fibre	[55]
25	2019-03	M-L	EDFL-AF-Ring	$Ti_3C_2T_x$	ACE	Spin Coating	D-shape fibre	[54]
26	2018-06	M-L	EDFL-AF-Ring	$Ti_3C_2T_x$	ACE	Immersion	Etched fibre	[100]
27	2018-01	M-L		Ti_3CNT_x	Interfacial technique	Solution Casting	Fibre ferrule	[36]
28	2017-11	M-L	YDFL-AF-Ring	$Ti_3C_2T_x$	ACE	Solution Deposition	D-shape fibre	[60]
		M-L	EDFL-AF-Ring	$Ti_3C_2T_x$	ACE	Solution Deposition	D-shape fibre	
29	2017-10	M-L	EDFL-AF-Ring	Ti_3CNT_x	ACE	Film Attached	D-shape fibre	[66]

4. Conclusion

Since conductors typically have poor SA properties, it is preferable to etch the terminating metallic element from the MAX phase material to create MXene. This is because nonlinear absorption is the most crucial factor in determining the effectiveness of pulse generation in both Q-switched and mode-locked passive-pulsed all-fibre lasers [98]. In particular, for all-fibre ring cavity lasers, the synthesis of MXene or MAX phases with exceptional nonlinear saturable absorption and adaptable grouping of $M_{n+1}X_nT_x$ helps with the realisation of superior SA by employing a variety of manufacturing and integration techniques and methodologies.

As a result, the creation of Q-switched and mode-locked pulsed all-fibre lasers is expected to move toward other untapped MXenes with many more well-studied material properties in the future. In order to corroborate the theoretical prediction, a highly relevant and accurate experimental bandgap measurement for the MXene is essential. This is because the importance of bandgap is often illustrated by matching the laser operating wavelength of the Q-switched and mode-locked laser.

Based on earlier studies, it was predicted that the bandgap of MXene would be smaller than 0.2 eV, especially for $Ti_3C_2T_x$ [26] and 0.81 eV for Nb_2C utilising the Tauc approach [70]. The truth is that even with enough modulation depth, high non-saturable loss SAs could not be used to create a mode-locked laser. In light of this, it is appropriate to discuss the significance of nonlinear saturable absorption and its effects on pulse performances in places where the factor of on-saturable loss was not addressed. It is also appropriate to emphasise the description of MXene SA's non-saturable loss in the study of MXene SAs. This parameter is crucial for describing the MXene SA's characteristics. Taking the example of V_2CT_x SAs, modulation depth decreased from nearly 90% down to below 30% as thickness of the film was increased from 11 nm to 116 nm [109]. On the other hand, the 73% non-saturable absorption loss in 116 nm thickness of V_2CT_x may not be enough to produce an effective fibre laser.

In addition to the significance of bandgap value, the most popular approach for the synthesis of MXene is the aqueous acid etching process. However, because the HF solution is extremely acidic, cautious handling methods and extra protection throughout the synthesis process are required. Since poor handling of the HF solution during the aqueous acid etching process—in the form of residue—may also cause serious contamination, electrochemical exfoliation is a more practical and secure alternative to AAE. To create MXene with improved stability, electrochemical exfoliation techniques use a highly fluorinated electrolyte which is a non-aqueous ionic liquid [75]. Another option to consider when working with materials whose bandgap value and stability during laser operation are unaffected by the removal of surface-terminating metallic elements is mechanical exfoliation of MAX phase materials. The most popular fibre platform for fabricating the SA is tapered fibre. However, most papers only discussed the tapered fibre's dimension without detailing on its adiabaticity that affects the dimension. For instance, a research study on the optimisation of strong evanescent fields and minimal loss tapered fibre with a short length would be fascinating [110].

It is scientifically advised in majority of these research works that the lifetime of MXene is increased if it is stored in restricted conditions, such as low temperature conditions as low as 5 °C to extend the lifetime [53]. Further research is required to improve the environmental stability and durability of synthetic MXene with its initial performances. MXene has to have better longevity and dependability so that it may be stored at room temperature.

The uniformity of the SA material particles across the host material will be influenced by the rate of flow and the potential fall distance during drop-casting and solution-casting, particularly in the PVA fusion method of fabrication, necessitating extra caution to ensure constant and consistent

dropping or casting of aqueous solutions. Particularly in the process of creating SA thin films, the vaporisation phase requires the same amount of care to be provided in terms of keeping it at complete rest and maintaining a constant temperature.

Concisely, this review paper describes the most recent advances in MAX phase, MXene, and SA synthesis for near- and mid-infrared pulsed-wave all-fibre lasers. Despite the fact that MAX phase and MXene are more recent than SWCNT, MWCNT, SWCNT, TMD, graphene, and other materials for SAs, their good nonlinear saturable absorption characteristics are extremely encouraging to function as a sustainable SA option. Table 1 contains a summary of all the research publications combined. The obstacles and difficulties encountered in the MAX phase SA synthesis field were then examined, and a number of recommendations were made to overcome these issues, demonstrating its potential for further development regarding this research topic. This study is anticipated to provide readers a better understanding of the most recent progress made by MXene or MAX phase SAs with mode-locked fibre lasers and its prospects for future use in both academic and commercial research. Few MXene and MAX phase materials were suggested as the SA up to this point, but $Ti_3C_2T_x$ is the MXene SA that has received the most investigation and experimentation. It was utilised without the terminal-metal T_x being removed. Its strong coefficient of nonlinear absorption, amazing depth of modulation of even up to 50%, and bigger efficient nonlinear absorption coefficient compared to other 2D materials are the causes of this tight bandgap. Then, a discussion follows on $Ti_3C_2T_x$ and other MXene synthesis as well as material characterisation.

The aqueous acid etching approach is often utilised for the synthesis of MXene, according to the study. Following that, these MXene or MAX phases were used as SAs on the fibre platform in all-fibre ring cavity configuration. Microfiber has been demonstrated in several shapes, including tapered fibre, D-shaped fibre, and etched fibre, which have superior heat dissipation mechanisms and a higher threshold of optical damage. These SA materials' nonlinear saturable absorption capabilities were then studied using either twin-detector or Z-scan measurement techniques. Based on these findings, the modulation depth and saturation intensity of each SA were determined. Finally, above mentioned SAs were inserted into the all-fibre laser cavity to give near-infrared passive mode-locking.

Acknowledgement
This research work is funded by the Ministry of Higher Education Malaysia under Fundamental Research Grant Scheme (FRGS/1/2020/TK0/UTM/02/46).

References

[1] Sharma, Utkarsh, Chang-Seok Kim, and Jin U. Kang. "Highly stable tunable dual-wavelength Q-switched fiber laser for DIAL applications." *IEEE Photonics Technology Letters* 16, no. 5 (2004): 1277-1279. https://doi.org/10.1109/LPT.2004.825991.

[2] Shephard, Jonathan D., Francois Couny, Phillip St J. Russell, Julian DC Jones, Jonathan C. Knight, and Duncan P. Hand. "Improved hollow-core photonic crystal fiber design for delivery of nanosecond pulses in laser micromachining applications." *Applied Optics* 44, no. 21 (2005): 4582-4588. https://doi.org/10.1364/AO.44.004582.

[3] Skorczakowski, M., J. Swiderski, Wiesław Pichola, Piotr Nyga, A. Zajac, M. Maciejewska, L. Galecki et al. "Mid-infrared Q-switched Er: YAG laser for medical applications." *Laser physics letters* 7, no. 7 (2010): 498. https://doi.org/10.1002/lapl.201010019

[4] Nelson, Laron E., D. J. Jones, K. Tamura, Hermann A. Haus, and E. P. Ippen. "Ultrashort-pulse fiber ring lasers." *Applied Physics B: Lasers & Optics* 65, no. 2 (1997). https://doi.org/10.1007/s003400050273.

[5] Soong, H. Kaz, and João Baptista Malta. "Femtosecond lasers in ophthalmology." *American journal of ophthalmology* 147, no. 2 (2009): 189-197. https://doi.org/10.1016/j.ajo.2008.08.026.

[6] Fermann, Martin E., and Ingmar Hartl. "Ultrafast fibre lasers." *Nature photonics* 7, no. 11 (2013): 868-874. https://doi.org/10.1038/nphoton.2013.280.

[7] Xu, C., and F. W. Wise. "Recent advances in fibre lasers for nonlinear microscopy." *Nature photonics* 7, no. 11 (2013): 875-882. https://doi.org/10.1038/nphoton.2013.284.
[8] Sakr, Hesham, Yong Chen, Gregory T. Jasion, Thomas D. Bradley, John R. Hayes, Hans Christian H. Mulvad, Ian A. Davidson, Eric Numkam Fokoua, and Francesco Poletti. "Hollow core optical fibres with comparable attenuation to silica fibres between 600 and 1100 nm." *Nature communications* 11, no. 1 (2020): 6030. https://doi.org/10.1038/s41467-020-19910-7.
[9] You, J. W., S. R. Bongu, Q. Bao, and N. C. Panoiu. "Nonlinear optical properties and applications of 2D materials: theoretical and experimental aspects." *Nanophotonics* 8, no. 1 (2018): 63-97. https://doi.org/10.1515/nanoph-2018-0106.
[10] Martinez, Amos, Mohammed Al Araimi, Artemiy Dmitriev, Petro Lutsyk, Shen Li, Chengbo Mou, Alexey Rozhin, Misha Sumetsky, and Sergei Turitsyn. "Low-loss saturable absorbers based on tapered fibers embedded in carbon nanotube/polymer composites." *APL Photonics* 2, no. 12 (2017). https://doi.org/10.1063/1.4996918.
[11] Boetti, Nadia Giovanna, Diego Pugliese, Edoardo Ceci-Ginistrelli, Joris Lousteau, Davide Janner, and Daniel Milanese. "Highly doped phosphate glass fibers for compact lasers and amplifiers: a review." *Applied Sciences* 7, no. 12 (2017): 1295. https://doi.org/10.3390/app7121295.
[12] Keller, Ursula, Kurt J. Weingarten, Franz X. Kartner, Daniel Kopf, Bernd Braun, Isabella D. Jung, Regula Fluck, Clemens Honninger, Nicolai Matuschek, and J. Aus Der Au. "Semiconductor saturable absorber mirrors (SESAM's) for femtosecond to nanosecond pulse generation in solid-state lasers." *IEEE Journal of selected topics in QUANTUM ELECTRONICS* 2, no. 3 (1996): 435-453. https://doi.org/10.1109/2944.571743.
[13] Liu, Xing, Qun Gao, Yang Zheng, Dong Mao, and Jianlin Zhao. "Recent progress of pulsed fiber lasers based on transition-metal dichalcogenides and black phosphorus saturable absorbers." *Nanophotonics* 9, no. 8 (2020): 2215-2231. https://doi.org/10.1515/nanoph-2019-0566.
[14] Ahmad, H., S. N. Aidit, N. A. Hassan, S. I. Ooi, and Z. C. Tiu. "Tunable mode-locked laser with micro-air gap cavity." *Optics & Laser Technology* 88 (2017): 222-225. https://doi.org/10.1016/j.optlastec.2016.09.016.
[15] Ahmad, Harith, Siti Nabila Aidit, Shok Ing Ooi, and Zian Cheak Tiu. "Mode-locked thulium-fluoride fibre laser with an adjustable pulse width using a nonlinear optical loop mirror." *Quantum Electronics* 49, no. 2 (2019): 111. https://doi.org/10.1070/QEL16770.
[16] Chernysheva, Maria, Aleksey Rozhin, Yuri Fedotov, Chengbo Mou, Raz Arif, Sergey M. Kobtsev, Evgeny M. Dianov, and Sergei K. Turitsyn. "Carbon nanotubes for ultrafast fibre lasers." *Nanophotonics* 6, no. 1 (2017): 1-30. https://doi.org/10.1515/nanoph-2015-0156.
[17] Eatemadi, Ali, Hadis Daraee, Hamzeh Karimkhanloo, Mohammad Kouhi, Nosratollah Zarghami, Abolfazl Akbarzadeh, Mozhgan Abasi, Younes Hanifehpour, and Sang Woo Joo. "Carbon nanotubes: properties, synthesis, purification, and medical applications." *Nanoscale research letters* 9 (2014): 1-13. https://doi.org/10.1186/1556-276X-9-393.
[18] Hasan, Tawfique, Zhipei Sun, Fengqiu Wang, Francesco Bonaccorso, Ping Heng Tan, Aleksey G. Rozhin, and Andrea C. Ferrari. "Nanotube–polymer composites for ultrafast photonics." *Advanced materials* 21, no. 38-39 (2009): 3874-3899. https://doi.org/10.1002/adma.200901122.
[19] Bao, Qiaoliang, Han Zhang, Yu Wang, Zhenhua Ni, Yongli Yan, Ze Xiang Shen, Kian Ping Loh, and Ding Yuan Tang. "Atomic-layer graphene as a saturable absorber for ultrafast pulsed lasers." *Advanced Functional Materials* 19, no. 19 (2009): 3077-3083. https://doi.org/10.1002/adfm.200901007.
[20] Vali, Mehran, Daryoosh Dideban, and Negin Moezi. "Silicene field effect transistor with high on/off current ratio and good current saturation." *Journal of Computational Electronics* 15 (2016): 138-143. https://doi.org/10.1007/s10825-015-0758-1.
[21] Lau, K. Y., and D. Hou. "Recent research and advances of material-based saturable absorber in mode-locked fiber laser." *Optics & Laser Technology* 137 (2021): 106826. https://doi.org/10.1016/j.optlastec.2020.106826.
[22] Liu, Wenjun, Lihui Pang, Hainian Han, Mengli Liu, Ming Lei, Shaobo Fang, Hao Teng, and Zhiyi Wei. "Tungsten disulfide saturable absorbers for 67 fs mode-locked erbium-doped fiber lasers." *Optics express* 25, no. 3 (2017): 2950-2959. https://doi.org/10.1364/OE.25.002950.
[23] Bikorimana, S., P. Lama, A. Walser, R. Dorsinville, S. Anghel, A. Mitioglu, A. Micu, and L. Kulyuk. "Nonlinear optical responses in two-dimensional transition metal dichalcogenide multilayer: WS 2, WSe 2, MoS 2 and Mo 0.5 W 0.5 S 2." *Optics express* 24, no. 18 (2016): 20685-20695. https://doi.org/10.1364/OE.24.020685.
[24] Liang, Liangbo, Jun Wang, Wenzhi Lin, Bobby G. Sumpter, Vincent Meunier, and Minghu Pan. "Electronic bandgap and edge reconstruction in phosphorene materials." *Nano letters* 14, no. 11 (2014): 6400-6406. https://doi.org/10.1021/nl502892t.
[25] Ma, Chunyang, Weichun Huang, Yunzheng Wang, Jordan Adams, Zhenhong Wang, Jun Liu, Yufeng Song et al. "MXene saturable absorber enabled hybrid mode-locking technology: a new routine of advancing femtosecond fiber lasers performance." *Nanophotonics* 9, no. 8 (2020): 2451-2458. https://doi.org/10.1515/nanoph-2019-0527.

[26] Naguib, Michael, Murat Kurtoglu, Volker Presser, Jun Lu, Junjie Niu, Min Heon, Lars Hultman, Yury Gogotsi, and Michel W. Barsoum. "Two-dimensional nanocrystals produced by exfoliation of Ti3AlC2." *Advanced materials* 23, no. 37 (2011): 4248-4253. https://doi.org/10.1002/adma.201102306.

[27] Nguyen, Van Hiep, Rassoul Tabassian, Saewoong Oh, Sanghee Nam, Manmatha Mahato, Pitchai Thangasamy, Araz Rajabi-Abhari, Won-Jun Hwang, Ashhad Kamal Taseer, and Il-Kwon Oh. "Stimuli-responsive MXene-based actuators." *Advanced Functional Materials* 30, no. 47 (2020): 1909504. https://doi.org/10.1002/adfm.201909504.

[28] Wang, Dongyi, Lili Wang, and Guozhen Shen. "Nanofiber/nanowires-based flexible and stretchable sensors." *Journal of Semiconductors* 41, no. 4 (2020): 041605. https://doi.org/10.1088/1674-4926/41/4/041605.

[29] Xie, Zhongjian, Yanhong Duo, Zhitao Lin, Taojian Fan, Chenyang Xing, Li Yu, Renheng Wang et al. "The rise of 2D photothermal materials beyond graphene for clean water production." *Advanced Science* 7, no. 5 (2020): 1902236. https://doi.org/10.1002/advs.201902236.

[30] Liu, Shuang, Xueting Pan, and Huiyu Liu. "Two-dimensional nanomaterials for photothermal therapy." *Angewandte Chemie* 132, no. 15 (2020): 5943-5953. https://doi.org/10.1002/anie.201911477.

[31] Zhang, Chuanfang, Linfan Cui, Sina Abdolhosseinzadeh, and Jakob Heier. "Two-dimensional MXenes for lithium-sulfur batteries." *InfoMat* 2, no. 4 (2020): 613-638. https://doi.org/10.1002/inf2.12080.

[32] Jhon, Young In, Joonhoi Koo, Babak Anasori, Minah Seo, Ju Han Lee, Yury Gogotsi, and Young Min Jhon. "Metallic MXene saturable absorber for femtosecond mode-locked lasers." *Advanced Materials* 29, no. 40 (2017): 1702496. https://doi.org/10.1002/adma.201702496.

[33] Feng, Jiangjiang, Xiaohui Li, Tianci Feng, Yamin Wang, Jie Liu, and Han Zhang. "Harmonic mode-locked Er-doped fiber laser by evanescent field-based MXene Ti3C2Tx (T= F, O, or OH) saturable absorber." *Annalen der Physik* 532, no. 1 (2020): 1900437. https://doi.org/https://doi.org/10.1002/andp.201900437.

[34] Wu, Q., X. Jin, S. Chen, X. Jiang, Y. Hu, Q. Jiang, L. Wu et al. "MXene-based saturable absorber for femtosecond mode-locked fiber lasers." *Optics express* 27, no. 7 (2019): 10159-10170. https://doi.org/10.1364/oe.27.010159.

[35] Dong, Yongchang, Sergii Chertopalov, Kathleen Maleski, Babak Anasori, Longyu Hu, Sriparna Bhattacharya, Apparao M. Rao, Yury Gogotsi, Vadym N. Mochalin, and Ramakrishna Podila. "Saturable absorption in 2D Ti3C2 MXene thin films for passive photonic diodes." *Advanced materials* 30, no. 10 (2018): 1705714. https://doi.org/10.1002/adma.201705714.

[36] Hantanasirisakul, Kanit, and Yury Gogotsi. "Electronic and optical properties of 2D transition metal carbides and nitrides (MXenes)." *Advanced materials* 30, no. 52 (2018): 1804779. https://doi.org/10.1002/adma.201804779.

[37] Jafry, A. A. A., N. Kasim, M. F. M. Rusdi, A. H. A. Rosol, R. A. M. Yusoff, A. R. Muhammad, B. Nizamani, and S. W. Harun. "MAX phase based saturable absorber for mode-locked erbium-doped fiber laser." *Optics & laser technology* 127 (2020): 106186. https://doi.org/10.1016/j.optlastec.2020.106186.

[38] Eklund, Per, Manfred Beckers, Ulf Jansson, Hans Högberg, and Lars Hultman. "The Mn+ 1AXn phases: Materials science and thin-film processing." *Thin Solid Films* 518, no. 8 (2010): 1851-1878. https://doi.org/https://doi.org/10.1016/j.tsf.2009.07.184.

[39] Ching, Wai-Yim, Yuxiang Mo, Sitaram Aryal, and Paul Rulis. "Intrinsic mechanical properties of 20 MAX-phase compounds." *Journal of the American Ceramic Society* 96, no. 7 (2013): 2292-2297. https://doi.org/10.1111/jace.12376.

[40] Zhou, Yanchun, and Zhimei Sun. "Electronic structure and bonding properties of layered machinable Ti 2 AlC and Ti 2 AlN ceramics." *Physical Review B* 61, no. 19 (2000): 12570. https://doi.org/10.1103/PhysRevB.61.12570.

[41] Jafry, Afiq Arif Aminuddin, Ahmad Haziq Aiman Rosol, N. Kasim, Ahmad Razif Muhammad, Riries Rulaningtyas, Moh Yasin, and Sulaiman Wadi Harun. "Soliton mode-locked pulse generation with a bulk structured MXene Ti 3 AlC 2 deposited onto a D-shaped fiber." *Applied Optics* 59, no. 28 (2020): 8759-8767. https://doi.org/10.1364/AO.403122.

[42] Ahmad, Harith, Rosli Ramli, Norhasliza Yusoff, Muhamad Zharif Samion, M. F. Ismail, L. Bayang, Siti Nabila Aidit, A. K. Zamzuri, and K. Thambiratnam. "155 nm-wideband and tunable q-switched fiber laser using an MXene Ti3C2TX coated microfiber based saturable absorber." *Laser Physics Letters* 17, no. 8 (2020): 085103. https://doi.org/10.1088/1612-202X/aba0bd.

[43] Ahmad, Harith, Hissah Saedoon M. Albaqawi, Norazriena Yusoff, Wu Yi Chong, and Moh Yasin. "Q-Switched Fiber Laser at $1.5~\mu $ m Region Using Ti 3 AlC 2 MAX Phase-Based Saturable Absorber." *IEEE Journal of Quantum Electronics* 56, no. 2 (2019): 1-6. https://doi.org/10.1109/JQE.2019.2949798.

[44] Ahmad, H., N. N. Ismail, S. N. Aidit, S. A. Reduan, M. Z. Samion, and N. Yusoff. "2.08 µm Q-switched holmium fiber laser using niobium carbide-polyvinyl alcohol (Nb2C-PVA) as a saturable absorber." *Optics Communications* 490 (2021): 126888. https://doi.org/10.1016/j.optcom.2021.126888.

[45] Ahmad, Harith, M. F. M. Azri, Siti Nabila Aidit, Norazriena Yusoff, A. K. Zamzuri, Muhamad Zharif Samion, S. Wang, Y. Wang, and J. K. Sahu. "1.3 µm passively Q-Switched bismuth doped fiber laser using Nb2C saturable absorber." *Optical Materials* 116 (2021): 111087. https://doi.org/10.1016/j.optmat.2021.111087.

[46] Sun, Guoqing, Ming Feng, Kang Zhang, Tianhao Wang, Yuanhao Li, Dongdong Han, Yigang Li, and Feng Song. "Q-Switched and Mode-Locked Er-doped fiber laser based on MAX phase Ti2AlC saturable absorber." *Results in Physics* 26 (2021): 104451. https://doi.org/10.1016/j.rinp.2021.104451.

[47] Dong, Li, Hongwei Chu, Ying Li, Xiaoyang Ma, Han Pan, Shengzhi Zhao, and Dechun Li. "Surface functionalization of Ta4C3 MXene for broadband ultrafast photonics in the near-infrared region." *Applied Materials Today* 26 (2022): 101341. https://doi.org/https://doi.org/10.1016/j.apmt.2021.101341.

[48] Rutkowski, Paweł, Jan Huebner, Dariusz Kata, Leszek Chlubny, Jerzy Lis, and Katarzyna Witulska. "Thermal properties and laser processing of hot-pressed materials from Ti–Al–C system." *Journal of Thermal Analysis and Calorimetry* 137 (2019): 1891-1902. https://doi.org/10.1007/s10973-019-08107-w.

[49] Mo, Yuxiang, Paul Rulis, and W. Y. Ching. "Electronic structure and optical conductivities of 20 MAX-phase compounds." *Physical Review B* 86, no. 16 (2012): 165122. https://doi.org/10.1103/PhysRevB.86.165122.

[50] Tallman, Darin J., Babak Anasori, and Michel W. Barsoum. "A critical review of the oxidation of Ti2AlC, Ti3AlC2 and Cr2AlC in air." *Materials Research Letters* 1, no. 3 (2013): 115-125. https://doi.org/10.1080/21663831.2013.806364.

[51] Gao, Lingfeng, Chunyang Ma, Songrui Wei, Artem V. Kuklin, Han Zhang, and Hans Ågren. "Applications of few-layer Nb2C MXene: narrow-band photodetectors and femtosecond mode-locked fiber lasers." *ACS nano* 15, no. 1 (2021): 954-965. https://doi.org/10.1021/acsnano.0c07608.

[52] Li, Jie, Zilong Zhang, Lin Du, Lili Miao, Jun Yi, Bin Huang, Yanhong Zou, Chujun Zhao, and Shuangchun Wen. "Highly stable femtosecond pulse generation from a MXene Ti 3 C 2 T x (T= F, O, or OH) mode-locked fiber laser." *Photonics Research* 7, no. 3 (2019): 260-264. https://doi.org/10.1364/prj.7.000260.

[53] Jiang, Xiantao, Shunxiang Liu, Weiyuan Liang, Shaojuan Luo, Zhiliang He, Yanqi Ge, Huide Wang et al. "Broadband nonlinear photonics in few-layer MXene Ti3C2Tx (T= F, O, or OH)." *Laser & Photonics Reviews* 12, no. 2 (2018): 1700229. https://doi.org/10.1002/lpor.201700229.

[54] Sun, Dan Dan, Qian Ku Hu, Jin Feng Chen, and Ai Guo Zhou. "First principles calculations of the relative stability, structure and electronic properties of two dimensional metal carbides and nitrides." *Key Engineering Materials* 602 (2014): 527-531. https://doi.org/10.4028/www.scientific.net/KEM.602-603.527

[55] Venkatkarthick, Radhakrishnan, Nadnudda Rodthongkum, Xinyu Zhang, Shanmin Wang, Prasit Pattananuwat, Yusheng Zhao, Riping Liu, and Jiaqian Qin. "Vanadium-based oxide on two-dimensional vanadium carbide MXene (V2O x@ V2CT x) as cathode for rechargeable aqueous zinc-ion batteries." *ACS Applied Energy Materials* 3, no. 5 (2020): 4677-4689. https://doi.org/10.1021/acsaem.0c00309.

[56] Ying, Guobing, Sankalp Kota, Andrew D. Dillon, Aaron T. Fafarman, and Michel W. Barsoum. "Conductive transparent V2CTx (MXene) films." *FlatChem* 8 (2018): 25-30. https://doi.org/10.1016/j.flatc.2018.03.001.

[57] Jhon, Young In, Young Min Jhon, and Ju Han Lee. "Nonlinear optics of MXene in laser technologies." *Journal of Physics: Materials* 3, no. 3 (2020): 032004. https://doi.org/10.1088/2515-7639/ab9f89

[58] Jhon, Young In, Joonhoi Koo, Babak Anasori, Minah Seo, Ju Han Lee, Yury Gogotsi, and Young Min Jhon. "Metallic MXene saturable absorber for femtosecond mode-locked lasers." *Advanced Materials* 29, no. 40 (2017): 1702496. https://doi.org/10.1002/adma.201702496.

[59] Wang, Hsiu-Wen, Michael Naguib, Katharine Page, David J. Wesolowski, and Yury Gogotsi. "Resolving the structure of Ti3C2T x MXenes through multilevel structural modeling of the atomic pair distribution function." *Chemistry of Materials* 28, no. 1 (2016): 349-359. https://doi.org/10.1021/acs.chemmater.5b04250

[60] Naguib, Michael, Joseph Halim, Jun Lu, Kevin M. Cook, Lars Hultman, Yury Gogotsi, and Michel W. Barsoum. "New two-dimensional niobium and vanadium carbides as promising materials for Li-ion batteries." *Journal of the American Chemical Society* 135, no. 43 (2013): 15966-15969. https://doi.org/10.1021/ja405735d

[61] Wang, Yiduo, Yingwei Wang, Keqiang Chen, Kun Qi, Tianyu Xue, Han Zhang, Jun He, and Si Xiao. "Niobium carbide MXenes with broad-band nonlinear optical response and ultrafast carrier dynamics." *ACS nano* 14, no. 8 (2020): 10492-10502. https://doi.org/10.1021/acsnano.0c04390.

[62] Huang, Yongda, Jian Zhou, Guanjie Wang, and Zhimei Sun. "Abnormally strong electron–phonon scattering induced unprecedented reduction in lattice thermal conductivity of two-dimensional Nb2C." *Journal of the American Chemical Society* 141, no. 21 (2019): 8503-8508. https://doi.org/10.1021/jacs.9b01742.

[63] Lin, Han, Shanshan Gao, Chen Dai, Yu Chen, and Jianlin Shi. "A two-dimensional biodegradable niobium carbide (MXene) for photothermal tumor eradication in NIR-I and NIR-II biowindows." *Journal of the American Chemical Society* 139, no. 45 (2017): 16235-16247. https://doi.org/10.1021/jacs.7b07818.

[64] Dall'Agnese, Yohan, Maria R. Lukatskaya, Kevin M. Cook, Pierre-Louis Taberna, Yury Gogotsi, and Patrice Simon. "High capacitance of surface-modified 2D titanium carbide in acidic electrolyte." *Electrochemistry Communications* 48 (2014): 118-122. https://doi.org/10.1016/j.elecom.2014.09.002.

[65] Yang, Fumei, Yanqi Ge, Teng Yin, Jia Guo, Feng Zhang, Xian Tang, Meng Qiu et al. "Ti3C2T x MXene Quantum Dots with Enhanced Stability for Ultrafast Photonics." *ACS applied nano materials* 3, no. 12 (2020): 11850-11860. https://doi.org/10.1021/acsanm.0c02369.

[66] Halim, Joseph, Maria R. Lukatskaya, Kevin M. Cook, Jun Lu, Cole R. Smith, Lars-Åke Näslund, Steven J. May et al. "Transparent conductive two-dimensional titanium carbide epitaxial thin films." *Chemistry of Materials* 26, no. 7 (2014): 2374-2381. https://doi.org/10.1021/cm500641a.

[67] Yang, Fumei, Yanqi Ge, Teng Yin, Jia Guo, Feng Zhang, Xian Tang, Meng Qiu et al. "Ti3C2T x MXene Quantum Dots with Enhanced Stability for Ultrafast Photonics." *ACS applied nano materials* 3, no. 12 (2020): 11850-11860. https://doi.org/10.1021/acsanm.0c02369.

[68] Wang, Zhenhong, Hongbo Li, Mulin Luo, Tenghui Chen, Xuefeng Xia, Hualong Chen, Chunyang Ma et al. "MXene photonic devices for near-infrared to mid-infrared ultrashort pulse generation." *ACS Applied Nano Materials* 3, no. 4 (2020): 3513-3522. https://doi.org/10.1021/acsanm.0c00241.

[69] Jafry, Afiq Arif Aminuddin, Ahmad Haziq Aiman Rosol, N. Kasim, Ahmad Razif Muhammad, Riries Rulaningtyas, Moh Yasin, and Sulaiman Wadi Harun. "Soliton mode-locked pulse generation with a bulk structured MXene Ti 3 AlC 2 deposited onto a D-shaped fiber." *Applied Optics* 59, no. 28 (2020): 8759-8767. https://doi.org/10.1364/AO.403122.

[70] X Yan, XiaoXin, Man Jiang, Erkang Li, Xin Kang, Zhaoyu Ren, Duidui Li, Tianqi Wang, and Baole Lu. "Tunable high-order harmonic and dual-wavelength mode-locking in Er-doped fiber laser based on Ti3C2T x-Mxene." *Applied Physics Express* 14, no. 1 (2021): 012009. https://doi.org/10.35848/1882-0786/abd5cc

[71] Ahmad, H., R. Ramli, N. Yusoff, S. A. Reduan, A. K. Zamzuri, and K. Thambiratnam. "Performance of Nb2C MXene coated on tapered fiber as saturable absorber for the generation of mode-locked erbium-doped fiber laser." *Infrared Physics & Technology* 114 (2021): 103647. https://doi.org/10.1016/j.infrared.2021.103647.

[72] Ahmad, Harith, Rizal Ramli, Nor Najwa Ismail, Siti Nabila Aidit, Norazriena Yusoff, and Muhamad Zharif Samion. "Passively mode locked thulium and thulium/holmium doped fiber lasers using MXene Nb2C coated microfiber." *Scientific reports* 11, no. 1 (2021): 11652. https://doi.org/10.1038/s41598-021-90978-x.

[73] Gao, Bo, Ying-Ying Li, Chun-Yang Ma, Yi-Qing Shu, Ge Wu, Bing-Kun Chen, Jia-Yu Huo, Ying Han, Lie Liu, and Ye Zhang. "Ta4C3 MXene as a saturable absorber for femtosecond mode-locked fiber lasers." *Journal of Alloys and Compounds* 900 (2022): 163529. https://doi.org/10.1016/j.jallcom.2021.163529.

[74] Khazaeinezhad, Reza, Sahar Hosseinzadeh Kassani, Hwanseong Jeong, Tavakol Nazari, Dong-Il Yeom, and Kyunghwan Oh. "Mode-locked all-fiber lasers at both anomalous and normal dispersion regimes based on spin-coated $\hbox {MoS} _ {2} $ nano-sheets on a side-polished Fiber." *IEEE Photonics Journal* 7, no. 1 (2014): 1-9. https://doi.org/10.1109/JPHOT.2014.2381656.

[75] Ng, E. K., K. Y. Lau, H. K. Lee, N. Mohd Yusoff, A. R. Sarmani, M. F. Omar, and M. A. Mahdi. "L-band femtosecond fiber laser based on a reduced graphene oxide polymer composite saturable absorber." *Optical Materials Express* 11, no. 1 (2021): 59-72. https://doi.org/10.1364/OME.404238.

[76] Ng, E. K., K. Y. Lau, H. K. Lee, MH Abu Bakar, Y. Mustapha Kamil, M. F. Omar, and M. A. Mahdi. "Saturable absorber incorporating graphene oxide polymer composite through dip coating for mode-locked fiber laser." *Optical Materials* 100 (2020): 109619. https://doi.org/10.1016/j.optmat.2019.109619.

[77] Yang, Fumei, Yanqi Ge, Teng Yin, Jia Guo, Feng Zhang, Xian Tang, Meng Qiu et al. "Ti3C2T x MXene Quantum Dots with Enhanced Stability for Ultrafast Photonics." *ACS applied nano materials* 3, no. 12 (2020): 11850-11860. https://doi.org/10.1021/acsanm.0c02369

[78] Wang, Chong, Ziyan Wu, Xiaohui Li, Jiangjiang Feng, Wenfeng Luo, Yanqi Ge, Mengjia Qu, Lirong Jing, and Tikang Shu. "MXene Ti3C2TX modulator for robust generation of soliton molecules." *ChemNanoMat* 6, no. 10 (2020): 1502-1506. https://doi.org/10.1002/cnma.202000314.

[79] Li, Guoru, Lingling Yang, Ruwei Zhao, Feifei Wang, Hongkun Nie, Ruihua Wang, Kejian Yang, Baitao Zhang, and Jingliang He. "Generation of a square-shaped pulse in mode-locked fiber lasers with a microfiber-based few-layer Nb 2 C saturable absorber." *Applied Optics* 59, no. 36 (2020): 11240-11245. https://doi.org/10.1364/AO.412165.

[80] Zapata, J. D., David Steinberg, Lúcia AM Saito, R. E. P. De Oliveira, A. M. Cárdenas, and EA Thoroh De Souza. "Efficient graphene saturable absorbers on D-shaped optical fiber for ultrashort pulse generation." *Scientific reports* 6, no. 1 (2016): 20644. https://doi.org/10.1038/srep20644.

[81] Cui, Yudong, Feifei Lu, and Xueming Liu. "Nonlinear saturable and polarization-induced absorption of rhenium disulfide." *Scientific reports* 7, no. 1 (2017): 40080. https://doi.org/10.1038/srep40080

[82] Khazaeinezhad, Reza, Sahar Hosseinzadeh Kassani, Hwanseong Jeong, Tavakol Nazari, Dong-Il Yeom, and Kyunghwan Oh. "Mode-locked all-fiber lasers at both anomalous and normal dispersion regimes based on spin-coated $\hbox {MoS} _ {2} $ nano-sheets on a side-polished Fiber." *IEEE Photonics Journal* 7, no. 1 (2014): 1-9., https://doi.org/10.1109/JPHOT.2014.2381656.

[83] Park, Nam Hun, Hwanseong Jeong, Sun Young Choi, Mi Hye Kim, Fabian Rotermund, and Dong-Il Yeom. "Monolayer graphene saturable absorbers with strongly enhanced evanescent-field interaction for ultrafast fiber laser mode-locking." *Optics express* 23, no. 15 (2015): 19806-19812. https://doi.org/10.1364/OE.23.019806.

[84] Jafry, Afiq Arif Aminuddin, Ahmad Haziq Aiman Rosol, N. Kasim, Ahmad Razif Muhammad, Riries Rulaningtyas, Moh Yasin, and Sulaiman Wadi Harun. "Soliton mode-locked pulse generation with a bulk structured MXene Ti 3 AlC 2 deposited onto a D-shaped fiber." *Applied Optics* 59, no. 28 (2020): 8759-8767. https://doi.org/10.1364/AO.403122.

[85] Wang, Shuai, Lei Li, Yu-feng Song, Ding-yuan Tang, De-yuan Shen, and Lu-ming Zhao. "Vector soliton and noise-like pulse generation using a Ti3C2 MXene material in a fiber laser." *Frontiers of Information Technology & Electronic Engineering* 22, no. 3 (2021): 318-324. https://doi.org/10.1631/FITEE.2000033.

[86] Jhon, Young In, Joonhoi Koo, Babak Anasori, Minah Seo, Ju Han Lee, Yury Gogotsi, and Young Min Jhon. "Metallic MXene saturable absorber for femtosecond mode-locked lasers." *Advanced Materials* 29, no. 40 (2017): 1702496. https://doi.org/10.1002/adma.201702496

[87] Cui, Nan, Xiaoguang Zhang, Wenbo Zhang, Xianfeng Tang, and Lixia Xi. "True equalization of polarization-dependent loss in presence of fast rotation of SOP." *Applied Sciences* 10, no. 11 (2020): 3844. https://doi.org/10.3390/app10113844.

[88] Kim, Jeong Je, Hyerim Kim, Chong Min Koo, Jae Ha Lee, Sang Bae Lee, and Kwanil Lee. "Femtosecond mode-locked fiber laser Using an etched optical fiber immersed in liquid Mxene as a saturable absorber." In *2018 23rd Opto-Electronics and Communications Conference (OECC)*, pp. 1-2. IEEE, 2018.

[89] Lee, Hyub, Won Sik Kwon, Jin Hwan Kim, Daewon Kang, and Soohyun Kim. "Polarization insensitive graphene saturable absorbers using etched fiber for highly stable ultrafast fiber lasers." *Optics Express* 23, no. 17 (2015): 22116-22122. https://doi.org/10.1364/OE.23.022116

[90] Schulze, Sven, Michel Wehrhold, and Carsten Hille. "Femtosecond-pulsed laser written and etched fiber Bragg gratings for fiber-optical biosensing." *Sensors* 18, no. 9 (2018): 2844. https://doi.org/10.3390/s18092844

[91] Schulze, Sven, Michel Wehrhold, and Carsten Hille. "Femtosecond-pulsed laser written and etched fiber Bragg gratings for fiber-optical biosensing." *Sensors* 18, no. 9 (2018): 2844. https://doi.org/10.3390/s18092844

[92] Owji, Erfan, Hossein Mokhtari, Fatemeh Ostovari, Behnam Darazereshki, and Nazanin Shakiba. "2D materials coated on etched optical fibers as humidity sensor." *Scientific Reports* 11, no. 1 (2021): 1771. https://doi.org/10.1038/s41598-020-79563-w.

[93] Kaur, Mandeep, Geoffrey Hohert, Pierre M. Lane, and Carlo Menon. "Fabrication of a stepped optical fiber tip for miniaturized scanners." *Optical Fiber Technology* 61 (2021): 102436. https://doi.org/10.1016/j.yofte.2020.102436.

[94] Yan, XiaoXin, Man Jiang, Erkang Li, Xin Kang, Zhaoyu Ren, Duidui Li, Tianqi Wang, and Baole Lu. "Tunable high-order harmonic and dual-wavelength mode-locking in Er-doped fiber laser based on Ti3C2T x-Mxene." *Applied Physics Express* 14, no. 1 (2021): 012009. https://doi.org/10.35848/1882-0786/abd5cc.

[95] Yang, Fumei, Yanqi Ge, Teng Yin, Jia Guo, Feng Zhang, Xian Tang, Meng Qiu et al. "Ti3C2T x MXene Quantum Dots with Enhanced Stability for Ultrafast Photonics." *ACS applied nano materials* 3, no. 12 (2020): 11850-11860. https://doi.org/10.1021/acsanm.0c02369.

[96] Nagai, Ryutaro, and Takao Aoki. "Ultra-low-loss tapered optical fibers with minimal lengths." *Optics express* 22, no. 23 (2014): 28427-28436. https://doi.org/10.1364/OE.22.028427.

[97] Jhon, Young In, Joonhoi Koo, Babak Anasori, Minah Seo, Ju Han Lee, Yury Gogotsi, and Young Min Jhon. "Metallic MXene saturable absorber for femtosecond mode-locked lasers." *Advanced Materials* 29, no. 40 (2017): 1702496. https://doi.org/10.1002/adma.201702496

[98] Venkatkarthick, Radhakrishnan, Nadnudda Rodthongkum, Xinyu Zhang, Shanmin Wang, Prasit Pattananuwat, Yusheng Zhao, Riping Liu, and Jiaqian Qin. "Vanadium-based oxide on two-dimensional vanadium carbide MXene (V2O x@ V2CT x) as cathode for rechargeable aqueous zinc-ion batteries." *ACS Applied Energy Materials* 3, no. 5 (2020): 4677-4689. https://doi.org/10.1021/acsaem.0c00309

[99] Dong, Li, Hongwei Chu, Ying Li, Xiaoyang Ma, Han Pan, Shengzhi Zhao, and Dechun Li. "Surface functionalization of Ta4C3 MXene for broadband ultrafast photonics in the near-infrared region." *Applied Materials Today* 26 (2022): 101341. doi: https://doi.org/10.1016/j.apmt.2021.101341.

[100] Jhon, Young In, Jinho Lee, Young Min Jhon, and Ju Han Lee. "Ultrafast mode-locking in highly stacked Ti3C2Tx MXenes for 1.9-μm infrared femtosecond pulsed lasers." *Nanophotonics* 10, no. 6 (2021): 1741-1751. https://doi.org/10.1515/nanoph-2020-0678.

[101] ENg, E. K., K. Y. Lau, H. K. Lee, MH Abu Bakar, Y. Mustapha Kamil, M. F. Omar, and M. A. Mahdi. "Saturable absorber incorporating graphene oxide polymer composite through dip coating for mode-locked fiber laser." *Optical Materials* 100 (2020): 109619. https://doi.org/10.1016/j.optmat.2019.109619.

[102] Jafry, Afiq Arif Aminuddin, Ahmad Haziq Aiman Rosol, N. Kasim, Ahmad Razif Muhammad, Riries Rulaningtyas, Moh Yasin, and Sulaiman Wadi Harun. "Soliton mode-locked pulse generation with a bulk structured MXene Ti 3 AlC 2

deposited onto a D-shaped fiber." *Applied Optics* 59, no. 28 (2020): 8759-8767. https://doi.org/10.1364/AO.403122.

[103] Ahmad, Harith, Hissah Saedoon M. Albaqawi, Norazriena Yusoff, Wu Yi Chong, and Moh Yasin. "Q-Switched Fiber Laser at $1.5~\mu $ m Region Using Ti 3 AlC 2 MAX Phase-Based Saturable Absorber." *IEEE Journal of Quantum Electronics* 56, no. 2 (2019): 1-6. https://doi.org/10.1109/JQE.2019.2949798.

[104] Wang, Zhenhong, Hongbo Li, Mulin Luo, Tenghui Chen, Xuefeng Xia, Hualong Chen, Chunyang Ma et al. "MXene photonic devices for near-infrared to mid-infrared ultrashort pulse generation." *ACS Applied Nano Materials* 3, no. 4 (2020): 3513-3522. https://doi.org/10.1021/acsanm.0c00241.

[105] Kaur, Mandeep, Geoffrey Hohert, Pierre M. Lane, and Carlo Menon. "Fabrication of a stepped optical fiber tip for miniaturized scanners." *Optical Fiber Technology* 61 (2021): 102436. https://doi.org/10.1016/j.yofte.2020.102436.

[106] Ying, Guobing, Sankalp Kota, Andrew D. Dillon, Aaron T. Fafarman, and Michel W. Barsoum. "Conductive transparent V2CTx (MXene) films." *FlatChem* 8 (2018): 25-30. https://doi.org/10.1016/j.flatc.2018.03.001

[107] Yan, XiaoXin, Man Jiang, Erkang Li, Xin Kang, Zhaoyu Ren, Duidui Li, Tianqi Wang, and Baole Lu. "Tunable high-order harmonic and dual-wavelength mode-locking in Er-doped fiber laser based on Ti3C2T x-Mxene." *Applied Physics Express* 14, no. 1 (2021): 012009. https://doi.org/10.35848/1882-0786/abd5cc

[108] Park, Nam Hun, Hwanseong Jeong, Sun Young Choi, Mi Hye Kim, Fabian Rotermund, and Dong-Il Yeom. "Monolayer graphene saturable absorbers with strongly enhanced evanescent-field interaction for ultrafast fiber laser mode-locking." *Optics express* 23, no. 15 (2015): 19806-19812. https://doi.org/10.1364/OE.23.019806

[109] Ying, Guobing, Sankalp Kota, Andrew D. Dillon, Aaron T. Fafarman, and Michel W. Barsoum. "Conductive transparent V2CTx (MXene) films." *FlatChem* 8 (2018): 25-30. https://doi.org/10.1016/j.flatc.2018.03.001

[110] Nagai, Ryutaro, and Takao Aoki. "Ultra-low-loss tapered optical fibers with minimal lengths." *Optics express* 22, no. 23 (2014): 28427-28436. https://doi.org/10.1364/OE.22.028427.

[111] Gao, Bo, Ying-Ying Li, Chun-Yang Ma, Yi-Qing Shu, Ge Wu, Bing-Kun Chen, Jia-Yu Huo, Ying Han, Lie Liu, and Ye Zhang. "Ta4C3 MXene as a saturable absorber for femtosecond mode-locked fiber lasers." *Journal of Alloys and Compounds* 900 (2022): 163529. https://doi.org/10.1016/j.jallcom.2021.163529.

[112] Yang, Fumei, Yanqi Ge, Teng Yin, Jia Guo, Feng Zhang, Xian Tang, Meng Qiu et al. "Ti3C2T x MXene Quantum Dots with Enhanced Stability for Ultrafast Photonics." *ACS applied nano materials* 3, no. 12 (2020): 11850-11860. https://doi.org/10.1021/acsanm.0c02369.